Fabrication of a Novel Glucose Biosensor Based on a Highly Electroactive Polystyrene/Polyaniline/Au Nanocomposite

Yuge Liu,[†] Xiaomiao Feng,[†,‡] Jianmin Shen,[†] Jun-Jie Zhu,[*,†] and Wenhua Hou[*,†]

School of Chemistry and Chemical Engineering, Key Laboratory of Analytical Chemistry for Life Science (MOE), Key Laboratory of Mesoscopic Chemistry (MOE), Nanjing University, Nanjing 210093, China, and Jiangsu Key Laboratory of Organic Electronics & Information Displays, Institute of Advanced Materials, Nanjing University of Posts and Telecommunications, Nanjing 210003, China

Received: March 5, 2008; Revised Manuscript Received: May 7, 2008

A novel nanocomposite with a core−shell structure containing polystyrene (PS), polyaniline (PANI), and Au nanoparticles (NPs) was synthesized. The nanocomposite was characterized by scanning electron microscopy (SEM), transmission electron microscopy (TEM), X-ray diffraction (XRD), X-ray photoelectron spectroscopy (XPS), and Fourier transform infrared spectroscopy (FTIR). Cyclic voltammetric experiments indicated that the nanocomposite had excellent redox ability in a wide range of pH values. The existence of Au NPs resulted in a higher electrical conductivity of the nanocomposite. As a model, glucose oxidase (GOD) was entrapped onto the nanocomposite-modified glassy carbon electrode (GCE) and applied to construct a sensor. The immobilized GOD showed a pair of well-defined redox peaks and high catalytic activity for the oxidation of glucose.

1. Introduction

The development of materials science and nanotechnology has brought a great momentum to bioelectroanalysis. Analysts in this field are always enthusiastic about finding new materials with good biocompatibility to improve the behavior of biosensors. Among these materials, conducting polymers have attracted much attention since the first report of electrical conductivity in a conjugated polymer.[1] These polymers are attractive materials for application in biosensors due to the considerable flexibility in their chemical structures and their redox characteristics. In recent years, great efforts have been made in the nanocomposites of conducting polymers and inorganic materials. These materials exhibit unique physical properties which are useful for the development of novel enzyme-based electrochemical biosensors with rapid electron transfer at the electrode surface. Much research has been reported on the application of the nanocomposites in biosensors.[2–5]

Polyaniline (PANI), one of the most important conducting polymers, has been widely applied in the field of biosensors. Different biomolecules such as enzyme, protein, and DNA have been successfully immobilized on the PANI-modified electrodes and showed excellent performances.[6–11] However, PANI is redox-active only under acidic conditions, generally when the solution pH is lower than 4.0,[12] and this greatly restricts its applications in biosensing. Moreover, in the doped conducting state, the insolubility of PANI in water also limits its applications.

Polystyrene (PS) latex beads are a kind of functional polymer material. These beads have many admirable properties such as biocompatibility, nontoxicity, high surface area, strong adsorption ability, and chemical inertness. PS latex beads have a high degree of hydrophilicity due to the negatively charged sulfate groups on their surface. The dispersibility of PANI in water can be greatly increased by combining PANI with PS.[13–15]

Metal nanoparticles (NPs) have been increasingly used in the fields of bioelectrochemical applications owing to their extraordinary electrocatalytic activity. Noble metal nanoparticles, especially Au NPs, have received considerable attention.[16–19] The electrical conductivity of PANI can be greatly increased if PANI is combined with Au NPs. The composites of PANI and Au NPs with a high electrical conductivity have been intensively investigated.[20–27] In spite of many reports on the composites of PANI with PS or Au NPs, few studies on the combination of these three components have been carried out, especially the application of the obtained nanocomposite in biosensors.

In this paper, a nanocomposite of PS/PANI/Au is synthesized. Combining with the advantages of PS, PANI, and Au NPs, the core−shell structured nanocomposite has many excellent properties, such as good solubility and dispersibility in water, satisfactory biocompatibility, and high electrical conductivity. The cyclic voltammetric results of the nanocomposite-modified glassy carbon electrode (GCE) indicated that this material was highly electroactive. The electrode showed redox activity in a wide pH range from 1.0 to 9.0. Due to the excellent electrochemical behavior and the good biocompatibility, the resultant nanocomposite is quite suitable for the construction of biosensors. As a model, glucose oxidase (GOD) was entrapped onto the nanocomposite-modified electrode. The direct electron transfer between GOD and the electrode can be easily realized and the enzyme exhibited bioactivity in solutions with a wide range of pH.

2. Experimental Section

2.1. Reagents. Aniline, styrene, ammonium persulfate ($(NH_4)_2S_2O_8$, APS), potassium persulfate ($K_2S_2O_8$, KPS), $HAuC1_4$, and trisodium citrate ($C_6H_5O_7Na_3 \cdot 2H_2O$) were purchased from Shanghai Chemical Reagent Company. Aniline and styrene were distilled under reduced pressure before use. Poly(sodium 4-styrenesulfonate) (PSS, $M_w \sim 70\,000$) was from

* To whom correspondence should be addressed. E-mail: jjzhu@nju.edu.cn (J.-J.Z.); whou@nju.edu.cn (W.H.). Phone/Fax: +86-25-8359-4976.
† Nanjing University.
‡ Nanjing University of Posts and Telecommunications.

10.1021/jp801938w CCC: $40.75
Published on Web 07/04/2008

Aldrich Chemical Co. GOD (Type VII from *Aspergillus nige*, 196 000 units/g of solid) was obtained from Sigma Chemical Co. and used as received. All other reagents were of analytical grade and used without further purification.

2.2. Synthesis of PS/PANI/Au Nanocomposite. Monodispersed PS beads with a diameter of 400 nm were prepared according to the literature.[28] The surface of PS colloid was first modified by PSS through a procedure described before.[29] For the preparation of core−shell structured PS/PANI, 4 mL of functionalized PS beads (about 1 g) was added into 16 mL of distilled water and then 1 mmol of aniline monomer was added into the suspension. After stirring for 30 min, 5 mL of 1 M HCl aqueous solution containing APS was dropped into the above mixture at room temperature. The molar ratio of aniline to APS was 1, and the reaction was allowed to proceed for 12 h. The final product was centrifuged and washed with distilled water and ethanol and then dried in a vacuum overnight at 40 °C.

The Au colloid was prepared by reducing $HAuC1_4$ aqueous solution with trisodium citrate.[30] The average diameter of the prepared Au NPs is about 20 nm. The electroactive three-component nanocomposite was synthesized by stirring the core−shell structured PS/PANI in Au colloid at a concentration of 1.0 mg/3.0 mL for 12 h. The resultant product was centrifuged and dried as that of the PS/PANI composite. It was found that Au NPs could be easily adsorbed on the surface of PS/PANI, resulting in the formation of PS/PANI/Au nanocomposite.

2.3. Preparation of a PS/PANI/Au Nanocompsite-Modified Glassy Carbon Electrode. GCE was first polished with 1.0, 0.3, and 0.05 μm alumina slurry successively and followed by rinsing with doubly distilled water and drying at room temperature. The PS/PANI/Au nanocomposite was dispersed in distilled water to form a 2.0 mg/mL solution under ultrasonication. The resultant colloidal solution (5 μL) was then dropped onto the pretreated electrode surface and allowed to dry under ambient conditions. For the direct electron transfer of GOD, 5 mg/mL GOD and 0.5% Nafion were subsequently cast onto the PS/PANI/Au nanocomposite-modified GCE and allowed to dry under ambient conditions for 2 h after each drop-casting step.

2.4. Characterization. The morphologies of the PS/PANI/Au nanocomposite were investigated by scanning electron microscopy (SEM, LEO1530VP) and transmission electron microscopy (TEM, JEOLJEM-200CX). X-ray diffraction (XRD) patterns were obtained on a Philip-X'Pert X-ray diffractometer. Fourier transform infrared (FTIR) spectroscopic measurements were taken on a Bruker model VECTOR22 Fourier transform spectrometer. The measurement of conductivity was realized by a four-probe method on a WR-2B digital multimeter using the compressed pellets of powders at room temperature. X-ray photoelectron spectroscopic (XPS) analysis was performed on an ESCALAB MK II X-ray photoelectron spectrometer.

Cyclic voltammetric and amperometric experiments were conducted with a CHI660B workstation (Shanghai Chenhua, Shanghai). All experiments were carried out using a conventional three-electrode system in 0.1 M phosphate buffer solution (PBS), where nanocomposite-modified GCE was used as the working electrode, a platinum wire as the auxiliary electrode and a saturated calomel electrode (SCE) as the reference electrode.

3. Results and Discussion

3.1. Characterization of the PS/PANI/Au Nanocomposite. The obtained PS latex beads are uniform in size and morphology with an average diameter of 400 nm and smooth surface (Figure 1A). However, the surface becomes rough after the polymerization of aniline, indicating the formation of PANI shell (Figure 1B). Figure 2 shows the typical TEM and SEM images of the PS/PANI/Au nanocomposite. The outside particles in Figure 2 are Au NPs. It can be clearly seen that the Au NPs are uniformly adsorbed onto the core−shell structured PS/PANI. The formation of the three-component nanocomposite can be described as follows. First, the surface of PS beads is modified with PSS in order to increase the negative charges. Then, aniline monomers can be adsorbed and further in situ polymerized on the surface of PS beads with the addition of oxidant, resulting in the formation of a PS/PANI core−shell structure. When the core−shell structured PS/PANI was introduced into the Au colloid, Au-decorated PS/PANI nanocomposite was formed by an electrostatic effect because the surface of citrate-stabilized Au NPs was electronegative.

The nature of the PS/PANI/Au nanocomposite was further proved by FTIR. As shown in Figure 3, all of the characteristic peaks of PANI are displayed. The peaks at 1581 and 1489 cm^{-1} can be ascribed to the C═C stretching vibrations of quinoid and benzenoid rings,[31] the peaks at 1302 and 1243 cm^{-1} are attributed to the C−N and C═N stretching modes,[32] and the

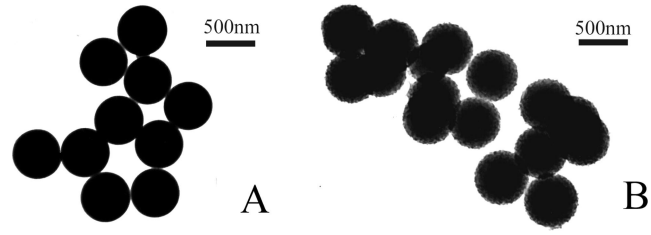

Figure 1. TEM images of (A) PS latex beads and (B) PS/PANI composite.

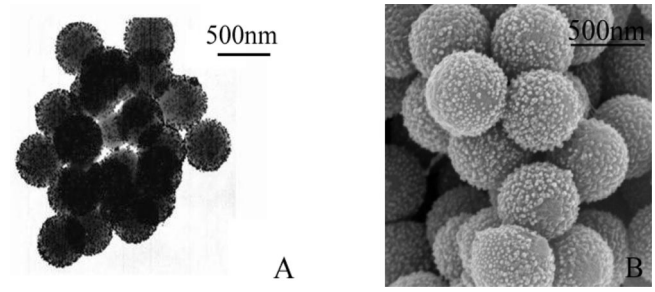

Figure 2. (A) TEM and (B) SEM images of the PS/PANI/Au nanocomposite.

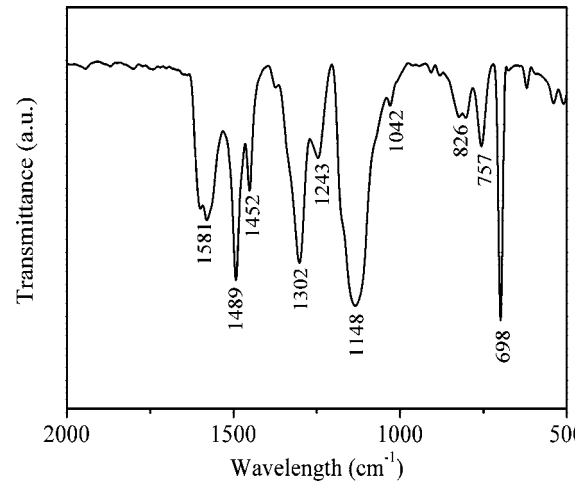

Figure 3. FTIR spectrum of the PANI/PS/Au nanocomposite.

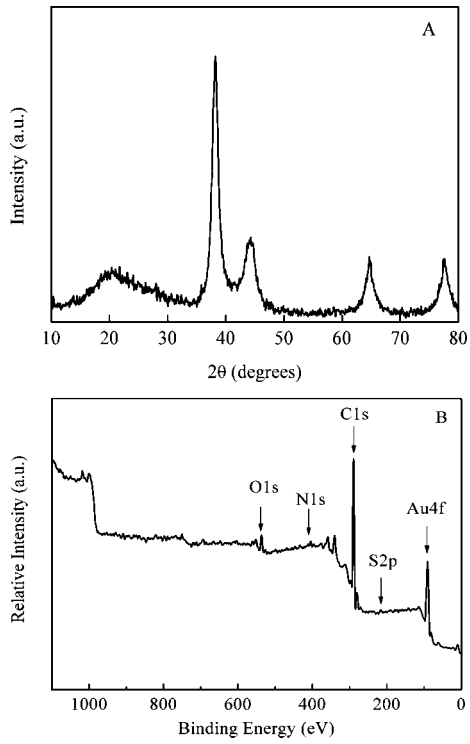

Figure 4. (A) XRD pattern and (B) XPS spectrum of the PS/PANI/Au nanocomposite.

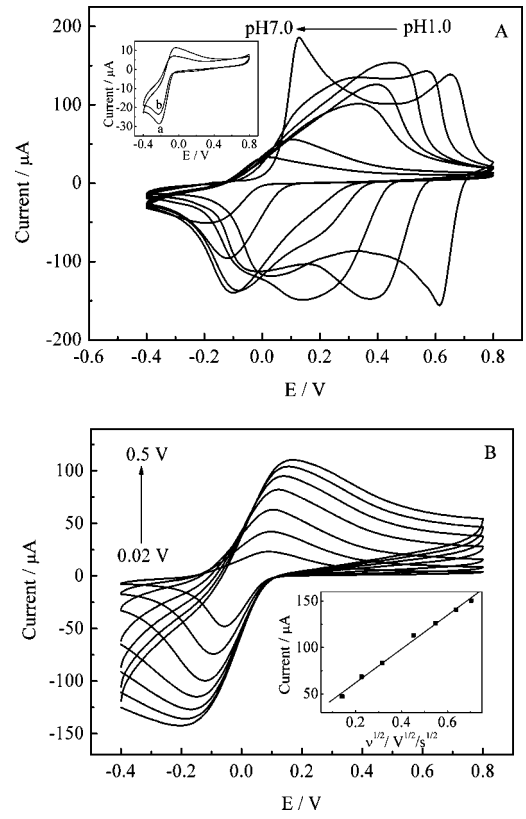

Figure 5. Cyclic voltammograms of (A) PS/PANI/Au nanocomposite-modified GCE measured in PBS with different pH values at 100 mV/s. Inset: PS/PANI/Au nanocomposite-modified GCE measured in (a) pH 8.0 and (b) pH 9.0 PBS. (B) PS/PANI/Au-modified GCE in pH 6.0 PBS at different scan rates: from inner to outside 20, 50, 100, 200, 300, 400, and 500 mV/s. Inset: calibration plot between the anodic peak current and the square root of the scan rate.

peaks at 1148 and 826 cm^{-1} are assigned to the in-plane and out-of-plane bending vibrations of C−H,[33,34] respectively. There is still a peak located at 1042 cm^{-1}, which belongs to the absorption of the $-SO_3H$ group of PSS. The typical adsorption bands of PS bands at 1452, 757, and 698 cm^{-1} can also be observed in Figure 3.

The XRD pattern of the PS/PANI/Au nanocomposite is displayed in Figure 4A. Besides the peak located at about a 2θ value of 22°, which can be assigned to the periodicity parallel to the polymer chains of PANI,[35] four additional peaks located at about 38, 44, 65, and 77° are observed after the reaction of PS/PANI with Au NPs. Those peaks represent the (111), (200), (220), and (311) Bragg reflections of Au. Moreover, XPS in a wide scan was also used for the characterization of the three-component nanocomposite. As can be seen in Figure 4B, a new peak at about 83.75 eV is observed besides the peaks of PS and PANI. This peak position can be assigned to Au 4f. It can be concluded that Au NPs exist in the nanocomposite.

The electrical conductivity of the PS/PANI composite is 2.09 $\times 10^{-3}$ S/cm, indicating that the composite forms a continuous phase. When Au NPs are adsorbed onto the surface of PS/PANI, the electrical conductivity of the three-component nanocomposite is increased to 7.54 $\times 10^{-3}$ S/cm. This can be ascribed to the excellent conducting performance of Au NPs. Therefore, the presence of Au NPs is favorable for the improvement of the electrical conductivity of PS/PANI.

3.2. Voltammetric Investigation. For pure PANI, it is only electroactive when the pH is lower than 4.0. However, when PANI is combined with PS latex beads and Au NPs, the electroactive ability is greatly improved. As shown in Figure 5A, the PS/PANI/Au nanocomposite-modified GCE shows redox peaks in solution with pH values from acid to neutral. It still has electroactivity even in PBS with a pH value of 9.0. The redox peaks observed in PBS from pH 5.0 to pH 9.0 are the overlap of two redox processes for PANI under acidic conditions. Generally, PANI exists in three well-defined oxidation states: leucoemeraldine, emeraldine, and pernigraniline. All of the nitrogen atoms are amines in the leucoemeraldine state and imines in the pernigraniline state, respectively. The ratio of amine to imine in emeraldine is almost 1. Emeraldine can be either in its base or salt form, depending on the pH value of the solution. The first and second oxidation waves correspond to the transition of leucoemeraldine to emeraldine salt and that of emeraldine salt to pernigraniline state in acid media, respectively.[29]

The effect of scan rate (υ) on the peak currents of the PS/PANI/Au nanocomposite-modified electrode in the range from 20 to 500 mV/s is shown in Figure 5B. With the increase of scan rate, the anodic peak potential shifts toward a more positive value and the cathodic peak potential shifts toward a more negative value. The anodic peak currents for PANI increase linearly with the square root of the scan rate ($\upsilon^{1/2}$), indicating that the peak current is diffusion-controlled.[36]

3.3. Entrapment of GOD onto the PS/PANI/Au Nanocomposite-Modified Electrode and Its Direct Electron Transfer. On the basis of the biocompatibility and the higher electrical conductivity, GOD was entrapped onto the PS/PANI/Au nanocomposite-modified electrode and the corresponding electrochemical properties were investigated in detail.

The cyclic voltammograms (CVs) of different electrodes are displayed in Figure 6. The PS/PANI/Au/Nafion-modified electrode does not show any obvious redox peaks, indicating that the Nafion membrane and the PS/PANI/Au nanocomposite are not electroactive in this potential range. After the entrapment of GOD, the PS/PANI/Au/GOD/Nafion-modified electrode

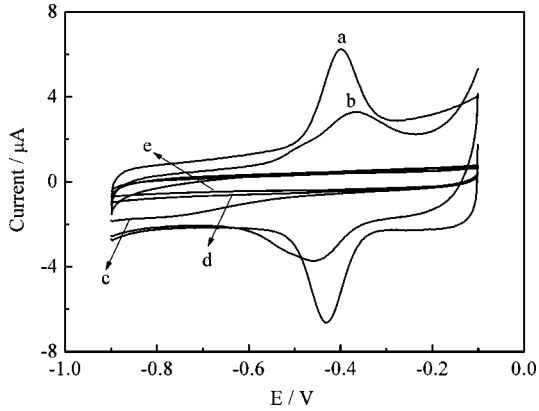

Figure 6. Cyclic voltammograms of (a) PS/PANI/Au/GOD/Nafion-, (b) PS/PANI/ GOD/Nafion-, (c) PS/PANI/Au/Nafion-, (d) Au/GOD/Nafion-, and (e) GOD/Nafion-modified GCE in 0.1 M air-free pH 6.0 PBS at 100 mV/s.

shows a pair of well-defined redox peaks at −0.39 and −0.43 V, respectively. These peaks result from direct electron transfer at the immobilized GOD for the conversion of GOD(FAD) to GOD($FADH_2$). There are still a couple of peaks on the PS/PANI/GOD/Nafion-modified electrode (Figure 6, curve b), but the peak currents are much smaller than those of the PS/PANI/Au/GOD/Nafion-modified electrode and the peak shape is not well-defined; this can be ascribed to the absence of Au NPs. The GOD/Nafion-modified electrode shows no peaks, which may be due to the very slow electron transfer of GOD at the electrode. Furthermore, despite the excellent conductivity of Au NPs, there exists nearly no peaks on the Au/GOD/Nafion-modified electrode (Figure 6, curve d). The reason may be that there is no carrier for Au NPs to realize its advantage in conducting. Thus, the PS/PANI/Au nanocomposite is very effective in the realization of the direct electron transfer of GOD molecules. It can be ascribed to the excellent conducting properties of the PS/PANI/Au nanocomposite.

The electrode shows a couple of well-defined peaks at different scan rates from as low as 20 to as high as 420 mV/s (see Supporting Information Figure S1). With the increase of scan rate, the redox peak currents of the GOD increase linearly (inset A of Supporting Information Figure S1), and so is the peak-to-peak separation, indicating a surface-controlled process. From Faraday's law, the average surface coverage of GOD is calculated to be 1.3×10^{-10} mol/cm^2. This value is much larger than that of 9.8×10^{-12} mol/cm^2 observed for the adsorption of GOD on Au NPs-modified carbon paste electrode and 1.54×10^{-11} mol/cm^2 observed for GOD/CdS-modified electrode.[37,38]

The CVs of PS/PANI/Au/GOD/Nafion-modified electrode show a strong dependence on the pH value of the solution (Figure 7). The formal potential shifts negatively with the increase of pH, and it exhibits a linear relationship over a wide pH range from 1.0 to 9.0 with a slope of 56.0 mV pH^{-1} (inset of Figure 7). This value is very close to the expected value of 58 mV pH^{-1}, indicating a two-proton process coupled with a two-electron transfer. It can be concluded that GOD exhibits excellent bioactivity in a very wide pH range, which has been rarely reported. This can be ascribed to the excellent electroactivity of PS/PANI/Au nanocomposite.

Small peak-to-peak separation always indicates a fast electron transfer rate. The electron transfer rate constant k_s can be estimated by the Laviron equation:[39]

$$k_s = mnFv/RT$$

where m is a parameter related to the peak-to-peak separation, T is the temperature, n is the number of electrons, v is the scan rate, F is the Faraday's constant, and R is the gas constant. The electron transfer rate constant k_s is estimated to be 4.63 ± 1.2 s^{-1} from this formula, which is much larger than that of Au NPs immobilized on Nafion film (1.3 s^{-1}),[40] and that of gold electrode modified with 3,3′-dithiobissulfocinnimidylpropionate (0.026 s^{-1}).[41] Therefore, the PS/PANI/Au nanocomposite can provide an excellent biocompatible environment for GOD and facilitate the electron transfer reaction.

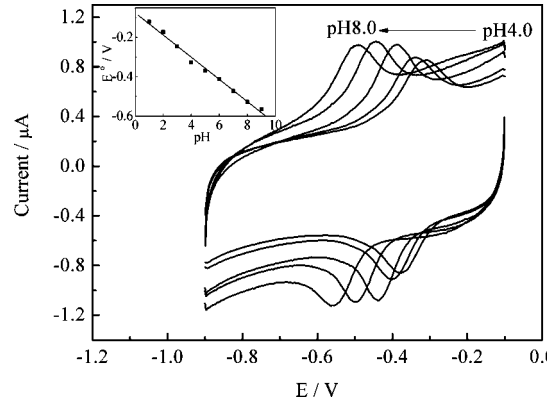

Figure 7. Cyclic voltammograms of PS/PANI/Au/GOD/Nafion-modified GCE in 0.1 M PBS with pH values of 4.0, 5.0, 6.0, 7.0, and 8.0 at 100 mV/s. Inset: plot of the formal potential vs pH.

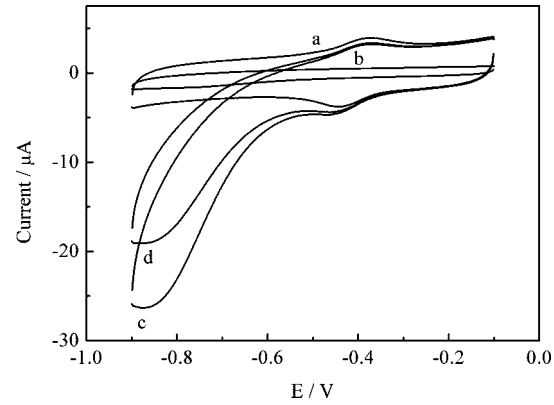

Figure 8. Cyclic voltammograms of (a) PS/PANI/Au/GOD/Nafion-modified electrode in nitrogen-saturated 0.1 M pH 6.0 PBS, (b) PS/PANI/Au/Nafion-modified electrode in air-saturated 0.1 M pH 6.0 PBS with 1 mM glucose, and PS/PANI/Au/GOD/Nafion-modified electrode in air-saturated PBS without glucose (c) and with 1 mM glucose (d) at 100 mV/s.

3.4. Applications of the PS/PANI/Au/GOD/Nafion-Modified Electrode in Biosensing. The CVs of PS/PANI/Au/GOD/Nafion-modified electrodes in nitrogen- and air-saturated 0.1 M pH 6.0 PBS solutions are given in Figure 8. A pair of well-defined redox peaks can be observed in both air- and nitrogen-saturated PBS. However, the reduction peak current is larger in air-saturated solution than that in nitrogen-saturated solution, which means that the electrochemically formed GOD($FADH_2$) can electrocatalyze the reduction of the dissolved oxygen.[38]

With the addition of glucose to the air-saturated solution, the PS/PANI/Au/Nafion-modified electrode shows no response (Figure 8, curve b), indicating that PS/PANI/Au cannot catalyze the oxidation of glucose. However, the reduction peak current decreases at the PS/PANI/Au/GOD/Nafion-modified electrode, indicating that GOD remains its bioelectrocatalytic activities and can catalyze the oxidation of glucose. The reduction peak current of the PS/PANI/Au/GOD/Nafion-modified electrode increases when H_2O_2 is added into air-free PBS (see Supporting Information Figure S2), indicating that the PS/PANI/Au/GOD/

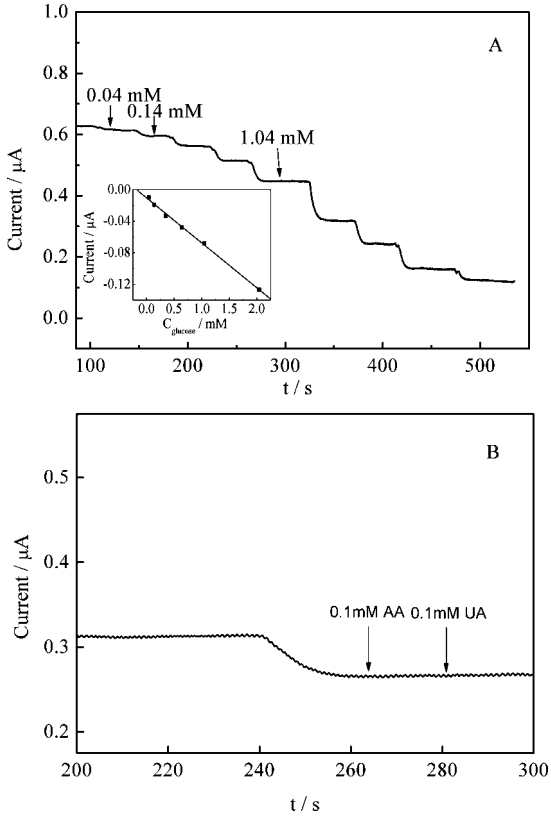

Figure 9. (A) Current−time curve of the PS/PANI/Au/GOD/Nafion-modified electrode for successive additions of specific concentrations of glucose to air-saturated 0.1 M pH 6.0 PBS under stirring at −0.38 V. Inset: Linear plot of current vs glucose concentration. (B) Effect of interfering species on biosensor response.

Nafion-modified electrode can catalyze the reduction of H_2O_2. Since GOD($FADH_2$) can generate H_2O_2 by reaction with the dissolved oxygen, the change in peak current is also the result of the reduction of H_2O_2. On the basis of the decrease of the electrocatalytic response to the dissolved oxygen, this system can be used to construct a glucose biosensor.

Shown in Figure 9A is a typical amperometric response curve of the biosensor through successive injections of glucose to stirring air-saturated pH 6.0 PBS. It can be clearly seen that the reduction current successively decreases with the addition of glucose. The biosensor achieved 90% of the steady-state current within 10 s, indicating a quick response process. The linear calibration range for glucose is 0.04−2.04 mM (inset of Figure 9A) with a detection limit of 12 μM at a signal-to-noise ratio of 3.

The apparent Michaelis−Menten constant K_m^{app}, which gives an indication of the enzyme−substrate kinetics, is generally used to evaluate the biological activity of immobilized enzyme. From the Lineweaver−Burk equation,[42] the apparent Michaelis−Menten constant was calculated to be 0.76 mM. This value is much smaller than 5.5 mM of GOD on gold−platinum alloy nanoparticles/multiwall carbon nanotubes[43] and 10.5 mM of GOD immobilized at chitosan and gold nanoparticles.[44] The smaller value of K_m^{app} indicates that the immobilized GOD entrapped on the PS/PANI/Au/GOD/Nafion-modified electrode possesses higher enzymatic activity, and the proposed electrode exhibits a higher affinity for glucose than other glucose biosensors.

The biosensor also shows a good selectivity for glucose. In an air-saturated and stirred 0.1 M pH 6.0 PBS containing 0.5 mM glucose, the response arising from 0.1 mM uric acid (UA) and ascorbic acid (AA) is negligible (Figure 9B).

Additional experiments were carried out to test the reproducibility and stability. No obvious change could be seen from the CV curves after 100 cyclic scans in pH 6.0 PBS at 100 mV/s. The biosensor was stored at 4 °C when not used, and it retained about 92% of its original bioactivity after half a month, indicating a good stability.

The relative standard deviation (RSD) of the peak current in six successive determinations at a glucose concentration of 0.1 mM was 2.6% for the PS/PANI/Au/GOD/Nafion-modified GCE. Five different modified GCEs were independently fabricated, and the corresponding RSD value determined at a glucose concentration of 0.2 mM was 4.5%.

4. Conclusions

In this paper, an electroactive core−shell structured PS/PANI/Au nanocomposite was synthesized. GCE modified by the resultant nanocomposite showed excellent redox ability in a wide pH range from 1.0 to 9.0. By incorporating Au NPs onto the surface of PS/PANI, the electrical conductivity was greatly improved. The nanocomposite-modified electrode not only realizes the direct electron transfer of GOD but also keeps its bioactivity in solutions from acidic to nearly alkaline. The biosensor constructed by the PS/PANI/Au/GOD/Nafion-modified electrode showed excellent response to glucose. This provides a facile way for the realization of direct electron of enzymes and has potential applications in biosening.

Acknowledgment. This work is supported by the National Natural Science Foundation of China (Nos. 20773065, 20635020, and 90606016), National Basic Research Program of China (No. 2007CB936302), and Modern Analysis Center of Nanjing University.

Supporting Information Available: Figures showing cyclic voltammograms of PS/PANI/Au/GOD/Nafion-modified GCE. This material is available free of charge via the Internet at http://pubs.acs.org.

References and Notes

(1) Shirakawa, H.; Louis, E. J.; MacDiarmid, A. G.; Chiang, C. K.; Heeger, A. J. *Chem. Commun.* **1977**, 577.
(2) Joshi, P. P.; Merchant, S. A.; Wang, Y.; Schmidtke, D. W. *Anal. Chem.* **2005**, *77*, 3183.
(3) Ali, S. R.; Ma, Y.; Parajuli, R. R.; Balogun, Y.; Lai, W. Y.-C.; He, H. *Anal. Chem.* **2007**, *79*, 2583.
(4) Yan, W.; Chen, X.; Li, X.; Feng, X.; Zhu, J.-J. *J. Phys. Chem. B* **2008**, *112*, 1275.
(5) Li, J.; Lin, X. *Biosens. Bioelectron.* **2007**, *22*, 2898.
(6) Kan, J.; Pan, X.; Chen, C. *Biosens. Bioelectron.* **2004**, *19*, 1635.
(7) Morrin, A.; Ngamna, O.; Kllard, A. J.; Moulton, S. E.; Smyth, M. E.; Wallace, G. G. *Electroanalysis* **2005**, *17*, 423.
(8) Oleg, A.; Raitman, E. K.; Andreas, F.; Bückmann, I. W. *J. Am. Chem. Soc.* **2002**, *124*, 6487.
(9) Forzani, E. S.; Zhang, H.; Nagahara, L. A.; Amlani, I.; Tsui, R.; Tao, N. *Nano Lett.* **2004**, *4*, 1785.
(10) Zhu, N.; Chang, Z.; He, P.; Fang, Y. *Electrochim. Acta* **2006**, *18*, 3758.
(11) Chang, H.; Yuan, Y.; Shi, N.; Guan, Y. *Anal. Chem.* **2007**, *79*, 5111.
(12) Tian, S.; Liu, J.; Zhu, T.; Knoll, W. *Chem. Mater.* **2004**, *16*, 4103.
(13) Aoki, K.; Chen, J.; Ke, Q.; Armes, S. P.; Randall, D. P. *Langmuir* **2003**, *19*, 5511.
(14) Lei, T.; Aoki, K.; Fujita, K. *Electrochem. Commun.* **2000**, *2*, 290.
(15) Barthet, C.; Armes, S. P.; Lascelles, S. F.; Luk, S. Y.; Stanley, H. M. E. *Langmuir* **1998**, *14*, 2032.
(16) Xiao, Y.; Pavlov, V.; Levine, S.; Niazov, T.; Markovitch, G.; Willner, I. *Angew. Chem., Int. Ed.* **2004**, *43*, 4519.
(17) Zayats, M.; Baron, R.; Popov, I.; Willner, I. *Nano Lett.* **2005**, *5*, 21.
(18) Raj, C. R.; Jena, B. K. *Chem. Commun.* **2005**, 2005.
(19) Zhong, C.-J.; Maye, M. M. *Adv. Mater.* **2001**, *13*, 1507.

(20) Tridib, K. S.; Devasish, C.; Anumita, P.; Arun, C. *Chem. Commun.* **2002**, 1048.
(21) Huang, K.; Zhang, Y.; Long, Y.; Yuan, J.; Han, D.; Wang, Z.; Niu, L.; Chen, Z. *Chem.—Eur. J.* **2006**, *12*, 5314.
(22) Feng, X.; Mao, C.; Yang, G.; Hou, W.; Zhu, J.-J. *Langmuir* **2006**, *22*, 4384.
(23) Feng, X.; Yang, G.; Xu, Q.; Hou, W.; Zhu, J.-J. *Macromol. Rapid Commun.* **2006**, *27*, 31.
(24) Long, Y.; Huang, K.; Yuan, J.; Han, D.; Niu, L.; Chen, Z.; Gu, C.; Jin, A.; Duvail, J. L. *Appl. Phys. Lett.* **2006**, *88*, 162113.
(25) Peng, Z.; Guo, L.; Zhang, Z.; Tesche, B.; Wilke, T.; Ogermann, D.; Hu, S.; Kleinermanns, K. *Langmuir* **2006**, *22*, 10915.
(26) Pillalamarri, S. K.; Blum, F. D.; Tokuhiro, A. T.; Bertino, M. F. *Chem. Mater.* **2005**, *17*, 5941.
(27) Sarma, T. K.; Chattopadhyay, A. *Langmuir* **2004**, *20*, 4733.
(28) Okubo, M.; ISE, E.; Yamashita, T. *J. Polym. Sci., Part A: Polym. Chem.* **1998**, *36*, 2513.
(29) Park, M.-K.; Onishi, K.; Locklin, J.; Caruso, F.; Advincula, R. C. *Langmuir* **2003**, *19*, 8550.
(30) Doron, A.; Katz, E.; Willner, I. *Langmuir* **1995**, *11*, 1313.
(31) Huang, K.; Wan, M. X. *Chem. Mater.* **2002**, *14*, 3486.
(32) McCarthy, P. A.; Huang, J.; Yang, S. C.; Wang, H. L. *Langmuir* **2002**, *18*, 259.
(33) Li, G. C.; Zhang, Z. K. *Macromolecules* **2004**, *37*, 2683.
(34) Trakhtenberg, S.; Hangun-Balkir, Y.; Warner, J. C.; Bruno, F. F.; Kumar, J.; Nagarajan, R.; Samuelson, L. A. *J. Am. Chem. Soc.* **2005**, *127*, 9100.
(35) Pillalamarri, S. K.; Blum, F. D.; Tokuhiro, S. T.; Story, J. G.; Bertino, M. F. *Chem. Mater.* **2005**, *17*, 227.
(36) Tian, S. J.; Baba, A.; Liu, J. Y.; Wang, Z. H.; Knoll, W.; Park, M.-K.; Advincula, R. *Adv. Funct. Mater.* **2003**, *13*, 473.
(37) Huang, Y. X.; Zhang, W. J.; Xiao, H.; Li, G. X. *Biosens. Bioelectron.* **2005**, *21*, 817.
(38) Liu, S. Q.; Ju, H. X. *Biosens. Bioelectron.* **2003**, *19*, 177.
(39) Laviron, E. *J. Electroanal. Chem.* **1979**, *101*, 19.
(40) Zhao, S.; Zhang, K.; Bai, Y.; Yang, W.; Sun, C. *Bioelectrochemistry* **2006**, *69*, 158.
(41) Jiang, L.; McNeil, C. J.; Cooper, J. M. *Chem. Commun.* **1995**, 1293.
(42) Kamin, R. A.; Wilson, G. S. *Anal. Chem.* **1980**, *52*, 1198.
(43) Kang, X.; Mai, Z.; Zou, X.; Cai, P.; Mo, J. *Anal. Biochem.* **2008**, *369*, 71.
(44) Wu, B.-Y.; Hou, S.-H.; Yin, F.; Li, J.; Zhao, Z.-X.; Huang, J.-D.; Chen, Q. *Biosens. Bioelectron.* **2007**, *22*, 838.

JP801938W